geosciences

Article

Evaluation of Remote Sensing Products for Wetland Mapping in the Irtysh River Basin

Kaiyue Luo [1,2,3], Alim Samat [2,3,4], Jilili Abuduwaili [2,3,4,*] and Wenbo Li [2,3,4]

1 College of Geography and Remote Sensing Science, Xinjiang University, Urumqi 830046, China; 107552203698@stu.xju.edu.cn
2 State Key Laboratory of Desert and Oasis Ecology, Key Laboratory of Ecological Safety and Sustainable Development in Arid Lands, Xinjiang Institute of Ecology and Geography, Chinese Academy of Sciences, Urumqi 830011, China; alim_smt@ms.xjb.ac.cn (A.S.); liwenbo212@mails.ucas.ac.cn (W.L.)
3 Research Center for Ecology and Environment of Central Asia, Chinese Academy of Sciences, Urumqi 830011, China
4 University of Chinese Academy of Sciences, Beijing 100049, China
* Correspondence: jilil@ms.xjb.ac.cn

Abstract: As a transboundary river with rich and unique wetland types, the Irtysh River faces various challenges and threats from human activities and climate change, which affect area, type, and function of wetland. To accurately obtain information on the spatial and temporal distribution of wetlands in this basin, this study compares and evaluates the consistency and accuracy of a total of eleven remote sensing (RS) based land use/land cover (LULC), and wetland products. The information extraction effect of each RS product was examined through methods such as wetland area and type description, thematic map comparison, and similarity coefficient and Kappa coefficient calculations, which can reflect the wetland distribution characteristics and differences among the RS products in the Irtysh River Basin. The results show that although there is a consensus among the products in the major wetland distribution areas, there are still obvious deviations in detail depiction due to differences in factors such as data sources and methods. The products of Global 30 m Wetland Fine Classification Data (GWL_FCS30) and Global 30 m Land Cover Data (GLC_FCS30-2020) released by the Institute of Space and Astronautical Information Innovation (ISAI) of the Chinese Academy of Sciences (CAS) have a clear advantage in extracting spatial morphology features of wetlands due to the use of multi-source data, while the Esri Global 10 m Land Cover Data (ESRI_Global-LULC_10m) and products such as the global 10 m land cover data (FROM_GLC10_2017) from Tsinghua University have higher classification consistency. Moreover, data resolution, classification scheme design, and validation methods are key factors affecting the quality of wetland information extraction in the Irtysh River Basin. In practical terms, the findings of this study hold significant implications for informed decision-making in wetland conservation and management within the Irtysh River Basin. By advancing wetland monitoring technologies and addressing critical considerations in information extraction, this research effectively bridges the gap between remote sensing technology and practical applications, offering valuable insights for regional wetland protection efforts.

Keywords: wetland; remote sensing; spatial and temporal distribution; consistency analysis; Irtysh River Basin

Citation: Luo, K.; Samat, A.; Abuduwaili, J.; Li, W. Evaluation of Remote Sensing Products for Wetland Mapping in the Irtysh River Basin. *Geosciences* **2024**, *14*, 14. https://doi.org/10.3390/geosciences14010014

Academic Editors: Jesus Martinez-Frias, Aggeliki Kyriou, Lia Bárbara Cunha Barata Duarte and Christos Pikridas

Received: 29 November 2023
Revised: 27 December 2023
Accepted: 29 December 2023
Published: 31 December 2023

1. Introduction

Wetlands are crucial ecosystems providing sustenance, water resources, and ecological services. They face imminent threats from human activities and climate change, making them the fastest shrinking ecosystems globally [1–6]. According to the findings by Nick C. Davidson, as documented in a comprehensive study on global wetland area changes, the long-term loss of natural wetlands is estimated to be within the range of 54–57% [7]. This meta-analysis, encompassing an examination of 189 reports detailing wetland alterations, further discerns a notably accelerated rate of wetland loss during the 20th and early 21st centuries, accounting for a discernible loss of 64–71% of wetlands since 1900 AD. These outcomes underscore significant challenges prevalent across diverse geographic regions, encompassing urban, coastal, inland, and plateau areas. These challenges materialize as observable reductions in wetland area, functional decline, habitat loss, biodiversity degradation, and heightened vulnerability of ecosystems [8–11]. Notably, wetland conservation and management exhibit pronounced disparities between developed and developing countries, influenced by policy, regulatory, and technical variations [12,13]. Additionally, diverse climate zones (e.g., temperate, tropical, boreal, etc.) contribute to significant differences in wetland response and adaptive capacity to climate change [14–16]. Wetlands are dynamic and complex ecosystems that vary significantly across different regions and climates. To effectively assess and monitor their status and trends, it is essential to obtain timely and accurate information on their spatial and temporal characteristics. RS technology has emerged as a powerful tool for this purpose, as it can provide large-scale and high-resolution data on wetland distribution and types. However, existing wetland RS products, predominantly global or continental scale, struggle to capture local variations and dynamics with high spatial and temporal resolutions. To address this limitation, accurate analysis of wetland characteristics in specific regions necessitates the application of RS methods for spatial and temporal distribution mapping.

In recent years, RS for wetland research has become a focal point, with numerous scholars and institutions worldwide conducting studies across various regions and scales [17–19]. These investigations, to varying degrees, reflect the diversity and complexity of wetlands. Notable examples include Julie Betbeder et al., who meticulously mapped the land cover of forested wetlands in the expansive "central depression" of Central Africa, constituting 32% of the region's total land area. Their study unraveled four distinct forested wetland types, shedding light on the intricate interplay between wetland types, flood extent, and phenology [20]. Turning attention to the globally significant Ramsar wetland along the coast of Turkey, Kuleli et al., conducted a comprehensive examination of shoreline change rates, revealing significant retreat and erosion in specific areas. Their findings underscore the need for robust conservation and management strategies for this internationally important wetland [21]. Following international wetland studies such as the coastal wetlands of Turkey, Wang et al., shifted their focus to the arid regions of China to investigate changes in wetland area in the Heihe River Basin. They found a subtle pattern of a decrease in wetland area from 2000 to 2014, followed by an increase. Nonetheless, the wetlands are still in a degraded state, which is the result of complex interactions between climate change and human activities [22]. Exploring the transformation of natural and artificial wetlands at the Yangtze River estuary, a vital hub for biodiversity and ecosystem services, Chen et al., [17] detected substantial changes. Over the period from 1960 to 2015, they noted a remarkable reduction of natural wetland area of 574.3 km^2, counterbalanced by a corresponding expansion of artificial wetland area by 553.6 km^2. The study highlighted the primary drivers behind this shift, primarily attributable to reclamation activities and sea level rise [23]. Collectively, these studies underscore the global importance of wetlands and demonstrate the utility of RS techniques in unraveling their dynamics and complexities.

The Irtysh River, a vital transboundary river integral to the Belt and Road Initiative, spans diverse countries and regions, significantly influencing both regional and global development [24,25]. Given its complex and variable climate, the Irtysh River Basin plays a crucial role in shaping hydrological cycles, ecosystem functions, and land use patterns [26]. The basin hosts various wetland types that provide essential ecological services, including food, water resources, and biodiversity. Meanwhile, these wetlands contribute to hydrological services such as water regulation, flood mitigation, and soil erosion control [27]. Despite their pivotal roles, the wetlands in this basin face an array of threats, including agricultural expansion, industrialization, urbanization, droughts, water resource development, and glacier melting [28]. The scarcity of RS studies on these wetlands underscores the pressing need for comprehensive RS research in the Irtysh River Basin.

Technological advancements of RS have yielded a plethora of global land cover and wetland products, each with varying spatial resolutions ranging from 30 m to 1° [29–31]. However, the existence of disparities in classification criteria and accuracy among these products necessitates a meticulous evaluation of their consistency. Focusing on the Irtysh River Basin, our study leverages eleven RS-based LULC and wetland products, each designed to reflect the spatiotemporal distribution characteristics of wetlands. The primary goal is to meticulously compare and assess the relative consistency and accuracy, focusing on relative metrics rather than absolute accuracy, of these products in describing wetlands. In doing so, we aim to explore their potential and limitations in the context of wetland conservation and management. To accommodate differences in classification systems, we implemented conversions and correspondences to ensure an accurate analysis of wetland characteristics.

This research not only provides a valuable reference for mapping wetland distribution in the Irtysh River Basin, but also aims to scrutinize the strengths and weaknesses of each RS product. Through a comprehensive assessment, we seek to understand their potential and limitations in wetland conservation and management from both accuracy and spatiotemporal perspectives. Additionally, we delve into the sources of errors and factors influencing RS product quality, proposing improvement measures and outlining future research directions. These findings not only offer crucial scientific support but also establish a solid decision-making basis for wetland conservation and management, aligning with the pursuit of sustainable development goals. It is worth mentioning that the list of all acronyms used in this paper is shown in Table 1.

Table 1. List of acronyms.

Acronyms	Definition
RS	Remote sensing
LULC	Land use/land cover
ISAI	Institute of Space and Astronautical Information Innovation
CAS	Chinese Academy of Sciences
GWL_FCS30	Global 30 m Wetland Fine Classification Data released by the ISAI of the CAS
GLC_FCS30-2020	Global 30 m Land Cover Data released by the ISAI of the CAS
ESRI_Global-LULC_10m	Esri Global 10 m Land Cover Data
FROM_GLC10_2017	The global 10 m land cover data from Tsinghua University
LCCS	Land Cover Classification System
UN-FAO	United Nations Food and Agriculture Organization
ESA	European Space Agency
JRC	European Union Joint Research Centre
OA	Overall Accuracy
EA	Expected Accuracy
GEE	Google Earth Engine

2. Materials and Methods

2.1. Study Area

Situated in the Northern Hemisphere and spanning approximately 165 × 104 km^2, the Irtysh River Basin (Figure 1) accommodates a population of approximately 15 million people, distributed across Mongolia (<1%), China (2.9%), Kazakhstan (53.1%), and Russia (44%) [32]. Originating from the southwest slope of the Altai Mountains in China, the Irtysh River is a transboundary watercourse that traverses Kazakhstan and Russia before discharging into the Arctic Ocean, covering a distance of 4248 km. The basin's geographical features significantly influence its wetlands and ecosystems, particularly in the upper reaches located in Xinjiang, China. The headwater part of the basin is characterized by high mountainous areas with permafrost and glaciers, as well as forest and grassland ecosystems. The long-term precipitation trend in the upper reach is relatively stable, ranging from 300–320 mm/year, which is considered the primary runoff generating area for the middle reach located in Kazakhstan [33]. The annual precipitation in the Irtysh River Basin is unevenly distributed, ranging from 400–650 mm/year in the mountainous and foothill areas of the northeastern part of the basin to less than 200 mm/year in the low-lying areas of the intermountainous terrain. The climate in the Irtysh River Basin varies from mountainous areas in the southeast to flat plains in the northwest, with average temperatures ranging from −12 °C to −19 °C in January and 20–22 °C in July [32].

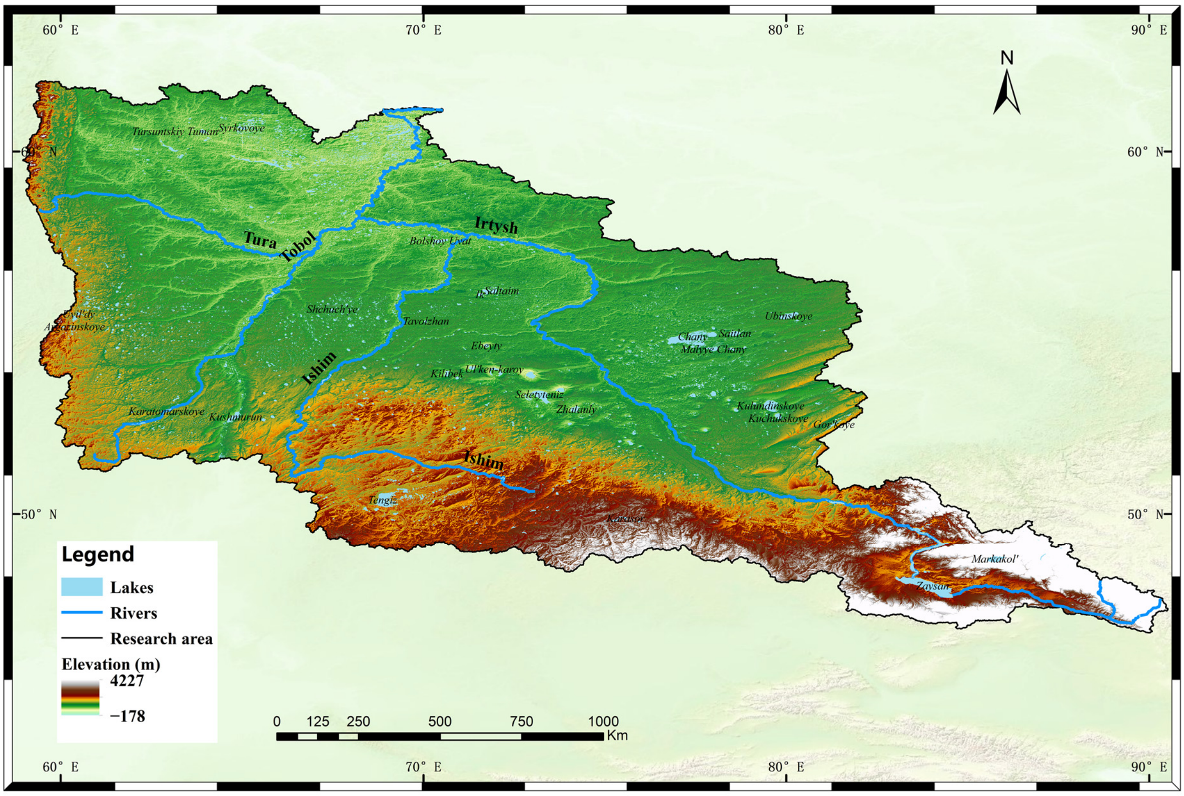

Figure 1. Map of the Irtysh River Basin. The elevations are represented relative to mean sea level, where negative values indicate heights below sea level. The legend's −178 m denotes areas with elevations lower than the reference sea level.

Amidst this diverse landscape, the Irtysh River Basin unveils its geological foundations, shaping its distinct features. Originating from the Altai mountain range, the upper reaches showcase a geological tapestry of crystalline Paleozoic complex meta-morphic rocks with magmatic intrusions. These formations not only shape the scenic terrain but serve as the primary source of both surface and groundwater for the entire catchment. As the river courses downstream, the terrain transforms into the flat expanse of the southern tip of the Siberian sedimentary basin. In the lower basin section, geological features shift, forming terraces closely hydraulically connected with the river. The Altai mountain range's Paleozoic volcanic and metamorphic rocks gradually yield to the immense sedimentary complex of the Siberian Basin, creating a smooth relief in the lower flat section—a stark contrast to the rugged upper reaches. Understanding these geological nuances is crucial as they delineate two distinctive sections within the Irtysh catchment. The upper mountainous part, characterized by crystalline rocks, serves as the wellspring of both surface and groundwater, shaping the hydrological dynamics of the entire basin. Conversely, the lower flat section, composed of sediments from the Siberian Basin, lacks significant tributaries, rendering it a relatively deficient environment from a water management perspective [34].

Wetlands within the Irtysh River Basin play crucial roles as integral components of the ecosystem, where they function as natural filters, providing habitats for biodiversity, sustaining ecological balance, and safeguarding water resources. Also, wetlands offer essential ecological services, including replenishing groundwater, regulating water quantity, mitigating floods, and controlling soil erosion. Their contributions extend to hydrological regulation and disaster prevention at the basin scale. Despite their ecological significance, these wetlands encounter formidable challenges and threats arising from human activities such as agriculture, industry, and urbanization, as well as the impacts of climate change. These pressures contribute to wetland degradation and destruction, leading to reductions in both wetland area and type, with adverse effects on wetland functions and biodiversity. The resultant degradation poses a significant threat to ecosystem health and may also precipitate economic and social challenges.

The imperative to comprehend wetland distribution and change within the Irtysh River Basin underscores the significance and value of this study. Evaluating the consistency and accuracy of wetland products is essential in this context. Precise acquisition of wetland information and analysis of wetland change trends provide insights into the current state and evolutionary processes of wetlands. Furthermore, this study establishes a scientific foundation for wetland conservation and management. Additionally, by promoting the application of RS technology in wetland monitoring and management, it contributes to enhancing the accuracy and reliability of wetland RS products. Ultimately, this research aligns with the pursuit of sustainable development goals.

2.2. Data Sources

2.2.1. GlobeLand30 V2020 Dataset

The GlobeLand30 V2020 dataset, developed by the National Geomatics Center of China, is a global land cover dataset with a 30 m resolution for the year 2020. This dataset incorporates multi-source RS images, including Landsat, HJ-1, and GF-1. Through image interpretation and classification algorithms, it encompasses 10 primary land cover types, including wetlands. The dataset boasts an overall accuracy of 85.72%, with a Kappa coefficient of 0.82 [35].

2.2.2. CGLS-LC100 Dataset

The CGLS-LC100 dataset, a global land cover change map with a 100 m resolution for 2019, is the product of the Copernicus Land Monitoring Service Global Team. Utilizing mainly PROBA-V satellite data and innovative algorithms, this dataset provides accurate and detailed information on land cover and use. Following the Land Cover Classification System (LCCS) of the United Nations Food and Agriculture Organization (UN-FAO), it encompasses 23 classification types, including wetland categories. The overall accuracy of the dataset is reported at 75% [36].

2.2.3. ESRI_Global-LULC_10m Dataset

Developed by Esri, the ESRI_Global-LULC_10m dataset is a global land use/land cover dataset with a 10 m resolution for 2020. Leveraging Sentinel-2 satellite data and deep learning models, the dataset comprises 10 primary classification types, including wetland categories. It offers detailed information on land use and cover for various applications such as conservation planning, food security, and hydrological models. The overall accuracy of the dataset is reported at 85% [37].

2.2.4. ESA WorldCover 10 m v100 Dataset

The ESA WorldCover 10 m v100 dataset, crafted by the European Space Agency (ESA), is a global land surface cover dataset with a 10 m resolution for 2020. Integrating Sentinel-1 and Sentinel-2 satellite data along with machine learning algorithms, the dataset includes

11 land surface cover categories, incorporating wetland categories. Consistent with the land surface cover classification system of the UN-FAO, it facilitates land use/land cover analysis on a global scale The overall accuracy of the dataset is reported at 75% [38].

2.2.5. GWL_FCS30 Dataset

The GWL_FCS30 dataset, developed by the Aerospace Information Innovation Institute of the Chinese Academy of Sciences, is a global wetland fine classification dataset with a 30 m resolution for 2020. Utilizing multi-source data and hierarchical adaptive models, this dataset covers nine wetland types in the Irtysh River Basin, providing detailed information on their spatial patterns and sub-class diversity. Notably, it excels in capturing the complexity and variability of wetlands The overall accuracy of the dataset is reported at 86% [39].

2.2.6. FROM_GLC10_2017 Dataset

The FROM_GLC10_2017 dataset, created by Tsinghua University, is a global land cover dataset with a 10-m resolution for 2017. Developed using Sentinel-2 satellite data and a random forest classifier, the dataset introduces the concept of stable classification, ensuring consistency in land cover types over time and space. With 10 land cover categories, it demonstrates an overall accuracy of 72.76%, offering increased spatial details and class separability compared to the 30 m Landsat-8 land cover map from the same team [40].

2.2.7. GLC_FCS30-2020 Dataset

Crafted by the Aerospace Information Innovation Institute of the Chinese Academy of Sciences, the GLC_FCS30-2020 dataset is a global land cover dataset with a 30 m resolution for 2020. Developed using Landsat time series images and an adaptive random forest model, this dataset encompasses 30 land cover types. Validated with 44,043 multi-source samples, it achieves an overall accuracy ranging from 68.7% to 82.5%, providing rich spatial and thematic details for regional or global analysis [41].

2.2.8. ESA CCI-LC Dataset

Developed by the European Space Agency, the ESA CCI-LC dataset is a global land cover dataset with a 300 m resolution for 2020. Based on multi-sensor satellite data, it offers consistent and comparable global land cover products from 1992 to 2020. Following the standardized classification system of the United Nations Food and Agriculture Organization, it encompasses 22 land cover types, with an average mapping accuracy of 71%. This dataset is valuable for analyzing regional-scale land use changes and supporting climate and ecological modeling for global change studies [42].

2.2.9. MCD12Q1 v061 Dataset

The MCD12Q1 dataset, developed by NASA, is a global land cover dataset with a 500 m resolution for 2021. Utilizing MODIS satellite data and employing data mining and machine learning algorithms, it distinguishes 17 land cover types. With an average accuracy of over 75%, the dataset is suitable for large-scale land use/cover change monitoring. Notably, it differentiates non-forest wetlands, such as swamps and river floodplains, from other land cover types, facilitating the analysis of spatiotemporal distribution and dynamics of wetlands and their interactions with other land uses [43].

2.2.10. GLC2000 Dataset

The GLC2000 dataset, developed by the European Union Joint Research Centre, is a global land cover dataset with a 1000 m resolution for the year 2000. Utilizing SPOT-4 satellite VEGETATION sensor images, the dataset adheres to the land cover classification system of the United Nations Food and Agriculture Organization, comprising 22 land cover types. Integrating other regional-scale land cover datasets, it applies standardized image classification methods to produce global land cover products, facilitating analysis of environmental issues such as land use change, biodiversity loss, and the carbon cycle [44].

2.2.11. AGLC-2015 Dataset

The AGLC-2015 dataset, developed by Sun Yat-sen University, is a land cover dataset with a 30 m resolution for 2015. Based on three global land cover products and data fusion methods, the dataset encompasses 10 types, including wetlands, with an overall accuracy of 76.10% and a Kappa coefficient of 0.72. Building upon AGLC-2015, the team also produced the global annual land cover dataset AGLC-2000-2015, providing data support for global change research and applications [45].

2.3. Data Pre-Processing

In order to facilitate a comprehensive comparison and analysis of wetland distribution across the eleven RS products and assess their accuracy, we executed the following pre-processing steps. Firstly, we extracted raster data corresponding to each RS product within the Irtysh River Basin, aligning with the vector boundary of the basin. Subsequently, we projected these raster datasets onto the WGS-84 coordinate system while preserving their original spatial resolution. Finally, thematic maps were generated for each RS product, retaining their specific wetland classification categories. Table 2 provides an overview of the key parameters associated with the eleven RS products.

The pre-processing steps were crucial to establish a standardized and consistent basis for comparison, enabling an accurate assessment of wetland distribution and RS product performance. Ensuring alignment to a common coordinate system and preserving the original spatial resolution were pivotal considerations for maintaining data integrity throughout subsequent analyses. The thematic mapping of raster data, with a specific focus on wetland classification categories, laid the foundation for a detailed and meaningful comparative evaluation. Table 2 provides essential parameters characterizing each RS product, offering readers a succinct reference to comprehend key attributes influencing subsequent analyses. This systematic approach to data pre-processing enhances the reliability and robustness of the comparative assessment, thereby contributing to the scientific rigor of our study.

2.4. Research Method

2.4.1. Descriptive Analysis of Wetland Areas and Types

(1) Wetland Category Selection

The objective of this study is to comprehensively assess the consistency and accuracy of eleven RS products in characterizing wetland features within the Irtysh River Basin, and the flowchart is shown in Figure 2. Additionally, we aim to discuss the potential and limitations of these RS products for effective wetland conservation and management. In pursuit of these goals, we identified wetland categories from the eleven RS products as the focal points of our analysis. These selected categories serve as representative indicators of the products' capabilities and characteristics in delineating wetland landscapes. Our primary research questions include: (1) How do different RS products exhibit variations in depicting the distribution and types of wetlands in the Irtysh River Basin? (2) What are the specific strengths and weaknesses associated with each RS product in describing wetlands? To address these questions, we initially curated a list of wetland categories for analysis, computed their respective areas within the study region, generated corresponding charts, and ultimately characterized the pattern of wetland distribution.

Table 2. Key information on the eleven RS-based LULC and wetland products.

Data Name	Primary Data Sources	Research and Development Organisations	Spatial Resolution/m	Vintages	Number of Classifications/pc	Data Sources
GlobeLand30 V2020	Landsat TM5/ETM+/OLI, HJ-1, GF-1	China National Centre for Basic Geographic Information	30	2020	10	http://www.globallandcover.com/ (accessed on 9 July 2023)
CGLS-LC100	External datasets such as PROBA-V, GeoWIKI, etc.	Copernicus Land Monitoring Service Global Team	100	2019	23	https://land.copernicus.eu/global/products/lc (accessed on 10 July 2023)
ESRI_Global-LULC_10m	Deep Learning Models and Training Datasets for ESA Sentinel-2, Impact Observatory	ESRI Corporation	10	2020	10	https://esri.maps.arcgis.com/ (accessed on 18 July 2023)
ESA WorldCover 10m v100	Sentinel-1/2 data, GeoWIKI samples	European Space Agency (ESA)	10	2020	11	https://viewer.esa-worldcover.org/worldcover/ (accessed on 10 July 2023)
GWL_FCS30	Landsat TM5/ETM+/OLI, Sentinel-1 SAR, ASTER GDEM	Institute of Space and Astronautical Information Innovation, Chinese Academy of Sciences	30	2020	9	https://zenodo.org/record/7340516 (accessed on 17 July 2023)
FROM_GLC10_2017	2015 30 m Landsat-8 data	Gong Peng Team, Tsinghua University	10	2017	10	http://data.starcloud.pcl.ac.cn/ (accessed on 16 August 2023)
GLC_FCS30-2020	Landsat time series imagery, CCI-LC products, MODIS NBAR data, 2014–2016	Institute of Space and Astronautical Information Innovation, Chinese Academy of Sciences	30	2020	30	https://data.casearth.cn/thematic/glc_fcs30 (accessed on 11 August 2023)
ESA CCI-LC	SPOT-VEGETATION images	European Space Agency (ESA)	300	2020	22	http://maps.elie.ucl.ac.be/CCI (accessed on 21 August 2023)
MCD12Q1 v061	MODIS data and other ground-based observations	NASA	500	2021	17	https://lpdaac.usgs.gov/products/mcd12q1v061/ (accessed on 17 August 2023)
GLC2000	SPOT-4 VEGETATION image	European Union Joint Research Centre (JRC)	1000	2000	28	https://forobs.jrc.ec.europa.eu/glc2000 (accessed on 21 August 2023)
AGLC-2015	Globeland30, FROM-GLC, and GLC-FCS30 products	Sun Yat-sen University	30	2015	10	https://doi.org/10.11834/jrs.20211261 (accessed on 18 August 2023)

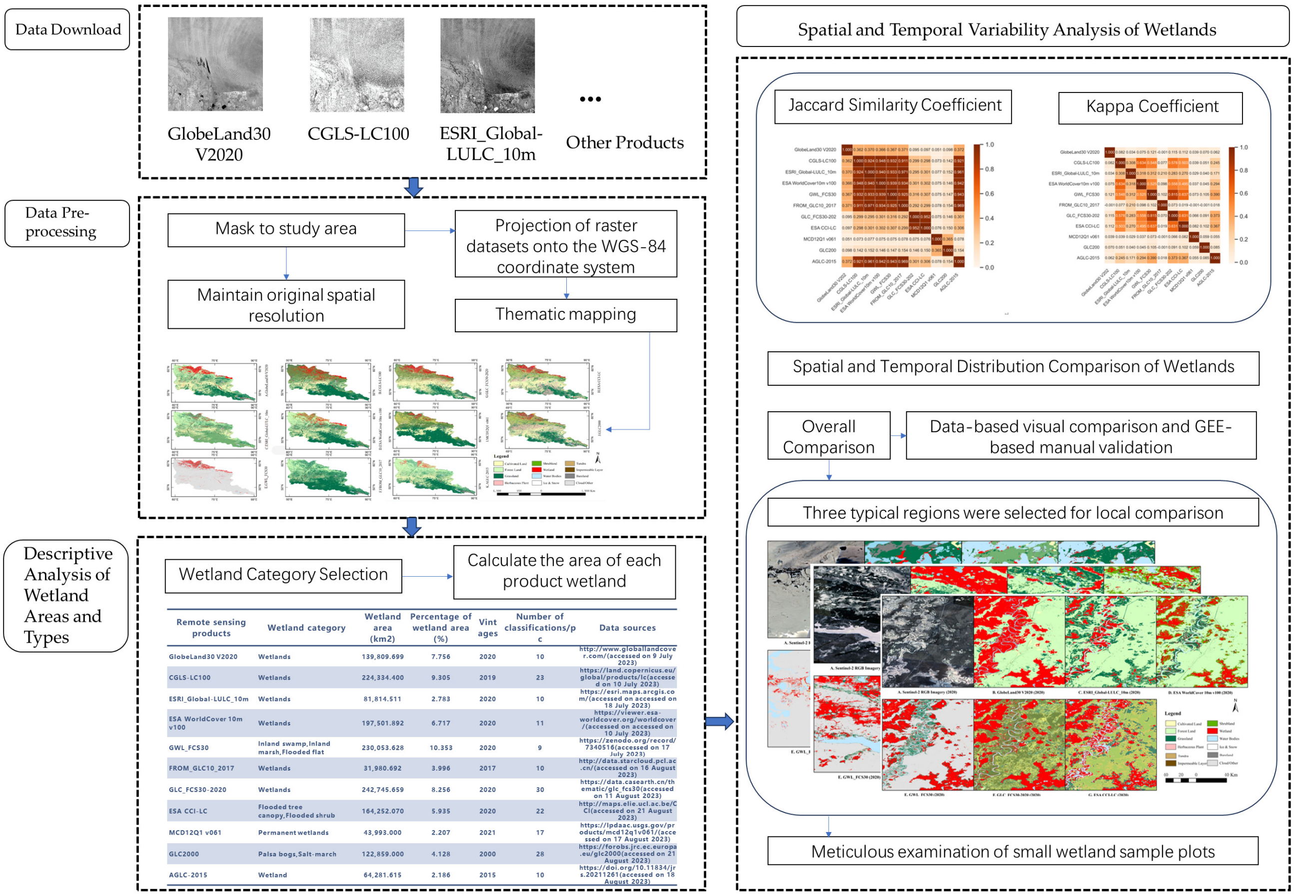

Figure 2. Research Flow Chart.

(2) Wetland Area Calculation

The area of each wetland category in the study area was determined using the following formula:

$$A_i = \frac{N_i \times R_i^2}{10^6} \tag{1}$$

where A_i is the wetland area of the i-th RS product (km^2), N_i is the number of pixels of the wetland category in the i-th product (pixel), and R_i is the spatial resolution of the i-th product (m).

The count of wetland pixels for each RS product was conducted using ArcGIS software. Subsequently, we multiplied this count by the square of the spatial resolution to obtain the area of each wetland category. The resulting data were organized into Table 3, and the percentage of each wetland category in the study area was calculated for further comparative analysis.

While this approach yields a reasonably precise estimation, it is not exempt from inherent limitations [46]. One notable constraint is the assumption that each pixel uniformly represents the same area. In reality, factors such as earth curvature and projection distortion can introduce variability in the area represented by each pixel, leading to potential errors in wetland area calculations. To remedy this limitation, future research could incorporate terrain correction models or pixel area normalization approaches to minimize variability introduced by earth curvature and projection distortion when calculating wetland areas.

Table 3. Area of each wetland category in the study area in eleven RS products.

Remote Sensing Product	Wetland Category	Wetland Area (km^2)	Percentage of Wetland Area (%)
GlobeLand30 V2020	Wetlands	139,809.699	7.756
CGLS-LC100	Wetlands	224,334.400	9.305
ESRI_Global-LULC_10m	Wetlands	81,814.511	2.783
ESA WorldCover 10 m v100	Wetlands	197,501.892	6.717
GWL_FCS30	Inland swamp, inland marsh, flooded flat	230,053.628	10.353
FROM_GLC10_2017	Wetlands	31,980.692	3.996
GLC_FCS30-2020	Wetlands	242,745.659	8.256
ESA CCI-LC	Flooded tree canopy, flooded shrub	164,252.070	5.935
MCD12Q1 v061	Permanent wetlands	43,993.000	2.207
GLC2000	Palsa bogs, salt-marsh	122,859.000	4.128
AGLC-2015	Wetland	64,281.615	2.186

(3) Wetland Distribution Description

Thematic maps of the eleven products within the study area were generated using ArcGIS software to facilitate the comparison and analysis of wetland distribution. Wetland-related categories were extracted from the raster data to focus specifically on wetland characteristics. Figure 3 illustrates the thematic maps of the eleven products in the Irtysh River Basin, where consistent colors denote identical land cover types, providing a visually accessible representation of their land cover distribution. These thematic maps serve as a means to observe the wetland classification outcomes of each RS product and discern the spatiotemporal distribution variations of wetlands among different RS products.

2.4.2. Spatial and Temporal Variability Analysis of Wetlands

To assess disparities in the spatial and temporal distribution of wetlands within the Irtysh River Basin across the eleven RS products, we employed two distinct methods.

(1) Jaccard Similarity Coefficient

The Jaccard similarity coefficient, a statistical metric quantifying the resemblance between two data sets, was utilized in this study [47]. It is defined as the proportion of the intersection over the union of two data sets:

$$J(A, B) = \frac{\mid A \cap B \mid}{\mid A \cup B \mid} \tag{2}$$

where A and B are two data sets, $\mid A \cap B \mid$ denotes the count of elements in their intersection, and $\mid A \cup B \mid$ indicates the count of elements in their union. The Jaccard coefficient ranges from 0 to 1, where 0 signifies no similarity whatsoever, and 1 denotes complete identity A higher value indicates a greater degree of similarity, whereas a lower value suggests less similarity.

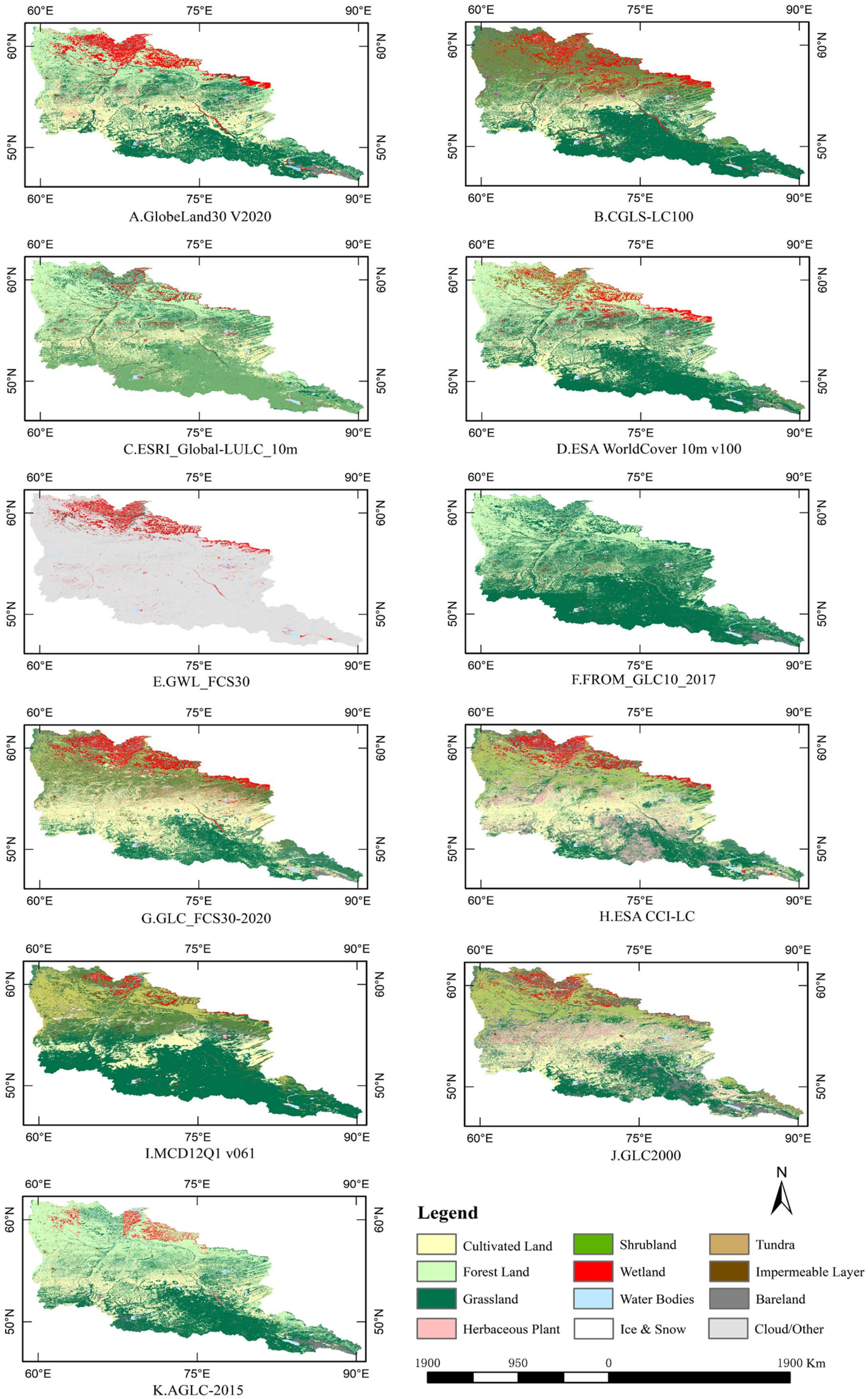

Figure 3. Thematic map of 11 categories of products in the Irtysh River Basin.

(2) Kappa Coefficient Analysis

The Kappa coefficient, a classification metric quantifying the agreement between two classification results [48], was employed in this study to compare the classification accuracy of each wetland category across the eleven RS products in the Irtysh River Basin. The methodology involves the following steps:

Firstly, the Overall Accuracy (OA), representing the ratio of matching pixels to the total number of pixels, was calculated from the confusion matrix using the formula:

$$OA = \frac{\sum_{i=1}^{n} X_{ii}}{\sum_{i=1}^{n} \sum_{j=1}^{n} X_{ij}} \tag{3}$$

where n denotes the number of wetland categories, and X_{ii} represents the element in row i and column i of the confusion matrix, indicating the number of matching pixels between category i in the reference data and category i in the comparison data. X_{ij} represents the element in row i and column j of the confusion matrix, indicating the number of matching pixels between class i in the reference data and class j in the comparison data. The order is determined by the rank order of the confusion matrix, not by the order of the reference and comparison data. The overall accuracy reflects the proportion of pixels of the same category in the two classification results, with a higher value indicating greater consistency.

Secondly, the Expected Accuracy (EA), representing the expected proportion of the number of pixels of the same category to the total number of pixels under the assumption of independence between the two categorization results, was computed based on the confusion matrix using the formula:

$$EA = \frac{\sum_{i=1}^{n} (\sum_{j=1}^{n} X_{ij})(\sum_{j=1}^{n} X_{ji})}{(\sum_{i=1}^{n} \sum_{j=1}^{n} X_{ij})^2} \tag{4}$$

where $\sum_{j=1}^{n} X_{ij}$ denotes the sum of elements in row i of the confusion matrix, i.e., the count of pixels of class i in the reference data. $\sum_{j=1}^{n} X_{ji}$ denotes the count of elements in column i of the confusion matrix, i.e., the count of pixels of class i in the comparison data. Expectation here refers to the theoretical value calculated according to the probabilities of random assignment, not the actual observed value.

Where $(\sum_{j=1}^{n} X_{ij})(\sum_{j=1}^{n} X_{ji})$ denotes the product of the counts of pixels in each class i in both reference and comparison data, i.e., the count of pixels that are identical in both according to the probability of random assignment. Summing such probabilities for all categories gives the expected accuracy. The expected accuracy reflects the proportion of pixels of the same category that two categorized results would have in a random situation, with smaller values indicating that they are less correlated.

Finally, the Kappa coefficient, the normalized difference between the overall accuracy and the expected accuracy, was derived from both values:

$$K = \frac{OA - EA}{1 - EA} \tag{5}$$

The Kappa coefficient ranges from -1 to 1, with -1 indicating complete disagreement, 0 indicating complete randomness, and 1 indicating complete agreement. It serves as a widely used measure of the level of agreement between two categorical outcomes after removing the random factor. Using this approach, Kappa coefficients were obtained between wetland categories in the eleven RS-based LULC and wetland products, quantifying their level of consistency in classifying wetlands in the Irtysh River Basin.

3. Results

3.1. Overview of Wetland Areas and Types

This section provides a comprehensive analysis and comparison of wetland area descriptions in the Irtysh River Basin across the eleven RS products. Table 3 presents data revealing substantial variations in the total wetland area, ranging from 64,281.615 km^2 to 230,053.628 km^2. These differences arise from distinct classification schemes, data sources, and production methods employed by the RS products. A visual representation of these disparities is illustrated in Figure 4a, depicted as a bar chart for enhanced clarity.

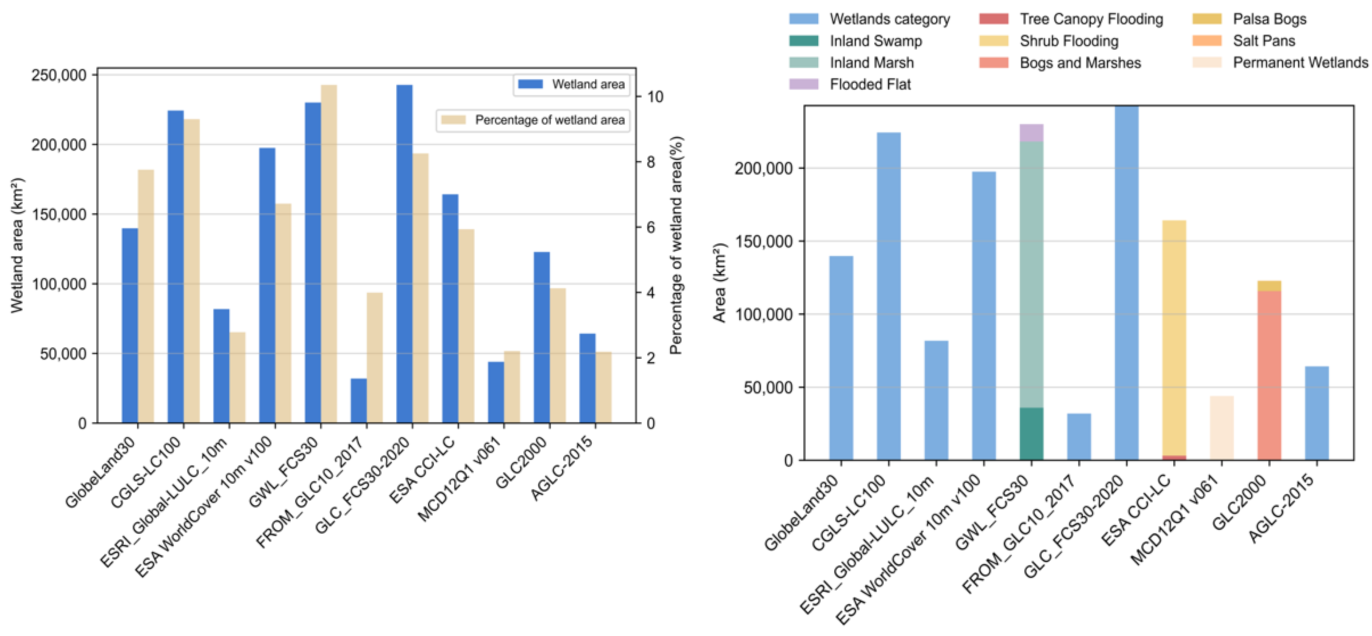

(**a**) (**b**)

Figure 4. Overview of Wetland Areas and Types. (**a**) Bar chart illustrating the differences in total wetland area among eleven RS products in the Irtysh River Basin. (**b**) Comparative representation of the area and percentage distribution of various wetland types across the eleven RS products.

Furthermore, a detailed examination of different wetland types is presented in Figure 4b, showcasing the area and percentage covered by each wetland type among the eleven RS products. Notably, some products, such as GlobeLand30 V2020, CGLS-LC100, ESRI_Global-LULC_10m, ESA WorldCover 10 m v100, FROM_GLC10_2017, GLC_FCS30-2020, MCD12Q1 v061, and AGLC-2015, exclusively describe one wetland type, encompassing wetlands, or permanent wetlands. Additionally, datasets like GWL_FCS30 describe three wetland types—inland swamp, swamp marsh, and flooded flat. The ESA CCI-LC dataset encompasses two wetland types—tree canopy flooding and shrub flooding. The GLC2000 dataset classifies wetlands into three categories—bogs and marshes, palsa bogs, and salt pans. These discrepancies can be attributed to variations in wetland definitions, classification accuracy, and data quality employed by the diverse RS products.

The systematic presentation of these findings establishes a robust foundation for understanding the diversity in wetland areas and types, laying the groundwork for subsequent detailed analyses and discussions in the following sections.

3.2. Assessment of Consistency and Accuracy of Wetland Products

This section undertakes a comprehensive comparison and evaluation of the spatiotemporal distribution of wetlands in the Irtysh River Basin using eleven RS products. Quantitative indicators are employed to assess the performance of these RS products in wetland description and classification, aiming to identify similarities, differences, and potential areas for improvement.

To begin, we computed the Jaccard similarity coefficient matrix for wetland categories among the different RS products (Figure 5). Key observations from this matrix include:

- ESRI_Global-LULC_10m and FROM_GLC10_2017 exhibit the highest agreement in wetland identification, with a Jaccard coefficient of 0.971. This alignment is attributed to the shared utilization of 10-m-resolution Sentinel-2 data and the application of deep learning models such as random forest model and Impact Observatory's deep learning AI land classification model in their classification processes;
- GlobeLand30 V2020 and MCD12Q1 v061 demonstrate the lowest agreement in wetland identification, featuring a Jaccard coefficient of only 0.051. This discrepancy is likely due to variations in data sources and classification schemes. GlobeLand30 V2020 utilizes multi-source data with 10 land cover classes, while MCD12Q1 v061 relies on MODIS data with 17 land cover classes and a resolution of 500 m;
- AGLC-2015 showcases a high degree of consistency, with a mean Jaccard coefficient of 0.595 across all products. This robust agreement is attributed to the data fusion strategy of AGLC-2015, integrating information from GlobeLand30, FROM-GLC, and GLC-FCS30,
- MCD12Q1 v061 exhibits lower agreement, with a mean Jaccard coefficient of 0.102. This could be due to its utilization of MODIS data at a resolution of 500 m and the application of data mining and machine learning algorithms for classification.

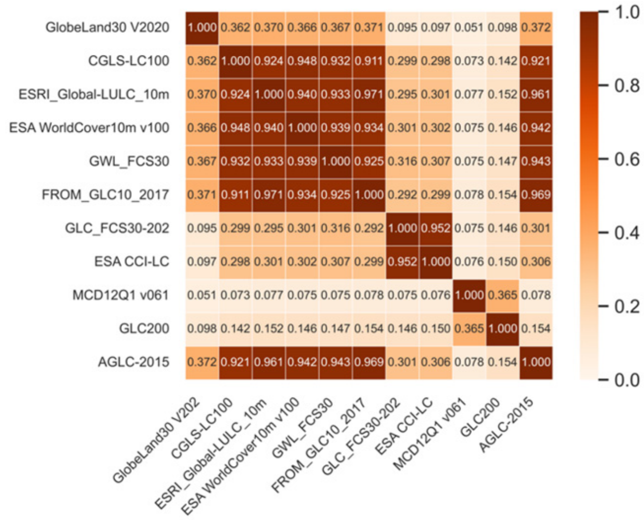

Figure 5. Jaccard similarity coefficient of wetland categories between different RS products.

The consistency of wetland RS products is influenced by factors such as data resolution, classification schemes, and methods [49–51]. These factors determine the applicability and accuracy of different products in defining, identifying, and describing wetlands. Selecting appropriate data sources and resolutions, along with designing rational classification schemes and methods, is crucial for improving the quality of wetland RS products. Considerations such as optical data susceptibility to clouds and fog, SAR data's ability to penetrate clouds, and the difficulty of terrain data in distinguishing vegetation types highlight the need for a balanced approach when choosing data sources and resolutions. Furthermore, the integration of multi-source data can enhance wetland identification results. Rational classification schemes and methods are pivotal for improving wetland description accuracy, necessitating a comprehensive evaluation of research scale and wetland types to strike a balance between detail and scope.

The use of the Jaccard similarity coefficient facilitates visual comparisons of the consistency in wetland identification among different RS products. This analysis, considering data resolution and methodology, serves as a valuable reference for the subsequent selection and enhancement of wetland RS products.

To further assess the consistency in wetland classification, Kappa coefficients between RS products were calculated (Figure 6). The Kappa coefficient, a key indicator measuring the level of agreement between classification results, provides insights into differences and reasons in wetland description.

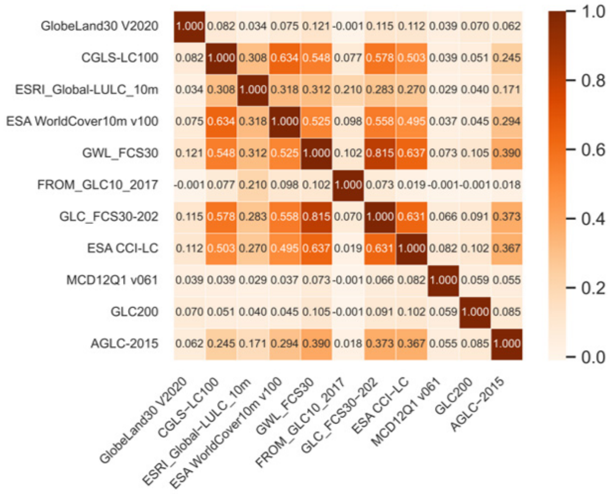

Figure 6. Kappa coefficients of wetland categories among RS products.

- Notably, the Kappa coefficient between GWL_FCS30 and GLC_FCS30-2020 is the highest at 0.815, indicating a robust consistency in wetland classification. This can be attributed to their detailed wetland classification system and hierarchical classification strategy, enabling the distinction of more wetland types and subtypes and capturing spatial details and changes,
- Conversely, the Kappa coefficients between FROM_GLC10_2017 and MCD12Q1 v061, FROM_GLC10_2017 and GLC2000, and FROM_GLC10_2017 and GlobeLand30 V2020 are the lowest, reaching only -0.001. This suggests a low consistency in wetland classification, potentially stemming from differences in data sources, resolutions, classification schemes, and methods, leading to deviations in wetland delineation and characterization.

Quantitative analysis of Kappa coefficients facilitates the evaluation of consistency among RS products in wetland classification, aiding in the identification of sources and factors contributing to errors. This analysis provides valuable guidance for the enhancement of wetland classification products, assisting both scientific and application fields in the selection and optimal use of RS products.

3.3. Spatial and Temporal Distribution Comparison of Wetlands

In this section, we rigorously assess the accuracy and consistency of various RS products in depicting wetlands within the Irtysh River Basin. Utilizing 3000 randomly generated points via the randomPoints function on the Google Earth Engine (GEE) platform, we conducted a representative and randomized assessment. Subsequently, we employed Google Earth high-resolution images to visually interpret each product's target year, following a common manual verification method. It is important to note that while effective, this approach may introduce subjective errors or uncertainties.

Upon conducting a comparative analysis of wetland distribution and types across the eleven RS products, we preliminarily assessed the degree of consistency between each product and the author's verification accuracy at the time of production. The observed distribution of each land cover closely aligned with the thematic map. Our comparative evaluation encompasses three aspects: overall, local, and detailed, offering methodological insights for subsequent wetland RS monitoring product selection, verification, and optimization.

(1) Overall Comparison

A comprehensive analysis of wetland area and type descriptions among the eleven RS products reveals significant diversity and discrepancies. Table 3 presents a range of total wetland area values, spanning from 64,281.615 km^2 to 230,053.628 km^2. These variations can be attributed to differences in data sources, classification schemes, and processing methods. Thematic maps in Figure 3 visually depict the concentration of wetlands extracted by different products in the middle and lower reaches of the Irtysh River Basin, with dense distribution along rivers and lakes.

Notably, the GWL_FCS30 product stands out for its proficiency in identifying small-scale wetlands, accurately delineating expansive wetland areas in the middle-eastern part, and successfully identifying scattered wetlands in the upstream mountainous area and southwestern part. This highlights the product's capability to capture diverse wetland features across different landscapes.

These findings underscore the importance of considering the specific strengths and limitations of each RS product in wetland analysis, as their performance can vary based on regional characteristics and the intended application. Figure 3 provides a visual representation of the spatial distribution, offering valuable insights for researchers and practitioners involved in wetland monitoring and management.

(2) Local Comparison

This refined comparative analysis, presented in Figure 7, aims to intricately evaluate wetland identification among six prominent remote sensing products (denoted as A to G), tailored for the year 2020 in the Irtysh River Basin, across three typical areas. The year 2020 is specifically emphasized because it is the most recent and comprehensive year for which data from multiple remote sensing products are available, and because it has important implications for wetland monitoring and conservation in the context of the United Nations Decades on Biodiversity and Ecosystem Restoration.

Among these products, the Sentinel-2 RGB Imagery (A) serves as a reference standard, providing high-resolution visual cues for wetland delineation. The remaining products, namely GlobeLand30 V2020 (B), ESRI_Global-LULC_10m (C), ESA WorldCover 10 m v100 (D), GWL_FCS30 (E), GLC_FCS30-2020 (F), and ESA CCI-LC (G), undergo a rigorous local comparison to discern their respective strengths and limitations within each of the three typical areas.

The comparative analysis of wetland localization in three typical areas of the Irtysh River Basin can effectively reveal subtle differences in wetland identification details between RS products. Through the analysis we can draw the following conclusions:

- GWL_FCS30 and GLC_FCS30-2020 products exhibit excellence in identifying small-scale and complex wetlands, showcasing their capability to capture spatial morphological details such as band or network distribution in swamp wetlands. However, GLC_FCS30-2020 may encounter instances of misclassification;
- The ESA WorldCover 10 m product excels in delineating wetland extension contours with higher accuracy;
- GlobeLand30 V2020 may exhibit misclassifications for certain land features,
- ESRI_Global-LULC_10m and ESA CCI-LC products may have difficulty identifying or misclassifying some fine wetland areas.

This localized comparative analysis, centered around the specifics of the Irtysh River Basin in 2020 and spanning three typical areas, refines our understanding of wetland dynamics. Furthermore, it offers valuable insights for the selection and optimization of remote sensing products in wetland monitoring applications, ensuring a more nuanced interpretation of wetland distribution and characteristics.

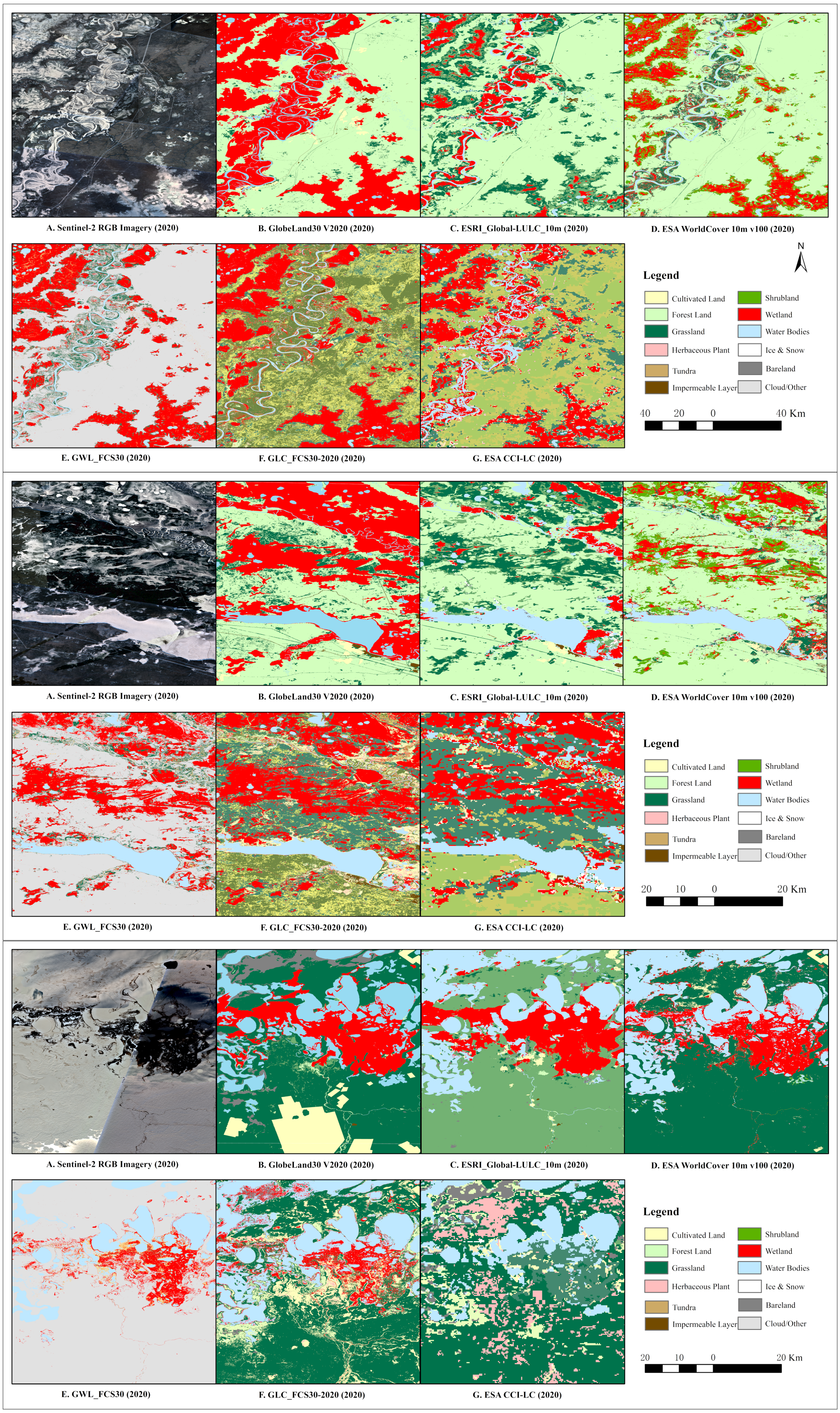

Figure 7. Comparative assessment of wetland identification in three typical areas of the Irtysh River Basin for the year 2020.

(3) Detailed Comparison

Upon meticulous examination of small wetland sample plots, distinct characteristics come to light. Wetland patches identified by the GWL_FCS30 and GLC_FCS30-2020 products exhibit smaller areas, greater numbers, and well-defined, continuous, and smooth boundaries. In contrast, wetland patches extracted by the ESRI-Global-LULC-10m and AGLC-2015 products feature relatively simplified boundaries, occasionally displaying omissions and misjudgments. These distinctions primarily arise from variations in wetland information classification and extraction algorithms between the two products.

The systematic assessment of spatial and temporal wetland distribution across the Irtysh River Basin contributes to a nuanced understanding of the strengths and weaknesses inherent in various RS products. This in-depth analysis serves as a foundation for informed decision-making in the selection and optimization of wetland RS monitoring products. The insights gained from this evaluation are invaluable for both scientific research and practical applications, providing a comprehensive perspective on the capabilities and limitations of different RS products in the context of wetland monitoring.

3.4. Factors Influencing Variances in Wetland Information Extraction

This section critically examines the principal factors contributing to disparities in wetland information extraction among the eleven RS products. The identified factors include data sources, spatial resolution, classification schemes, classification algorithms, and validation methods. These factors introduce variability in RS products' wetland descriptions, necessitating a thoughtful selection process aligned with research objectives while acknowledging inherent product characteristics and limitations. Simultaneously, enhancing the quality of RS products is crucial to support effective wetland conservation and management.

(1) Characteristics of Data Sources

The distinctiveness of land cover types is determined by the characteristics of data sources. Optical data susceptibility to clouds and fog, SAR data vulnerability to terrain influences, and terrain data sensitivity to source accuracy and processing methods underscore the need for preprocessing and correction measures.

(2) Spatial Resolution

Spatial resolution plays a pivotal role in delineating the level of detail and spatial variability in RS products. Higher-resolution data afford the capacity to distinguish more wetland subtypes and spatial patterns, while lower-resolution data can only capture broader wetland categories and large-scale changes. Selecting an appropriate spatial scale is therefore imperative.

(3) Classification Schemes and Algorithms

The core technologies underpinning RS product generation are classification schemes and algorithms, shaping the expression and granularity of land cover information. Variations in these components may lead to differences in naming, division, and attribution of identical land feature types. Intelligent classification methods such as deep learning, and optimization steps introduce further complexity. When utilizing RS products employing diverse classification schemes and algorithms, careful consideration is warranted to understand their impact on wetland type identification and differentiation, necessitating conversion and comparison procedures.

(4) Validation Methods

Validation methods represent a critical step in evaluating the quality and accuracy of RS products. Divergent validation methods can yield disparate accuracy assessment results for the same RS product. Considerations such as sample distribution, rigor, and cross-validation with other products or datasets are pivotal. When working with RS products employing distinct validation methods, it is essential to account for their influence on wetland accuracy assessment results, prompting calibration and adjustment efforts.

(5) Strengths and Weaknesses of Considered RS Products

Distinct RS products exhibit varying strengths and weaknesses in wetland description based on factors like data sources, spatial resolution, classification schemes, algorithms, and validation methods. Tailoring their usage to specific scenarios and wetland monitoring objectives is paramount. For instance, GlobeLand30 V2020, with its high resolution (30 m) and updated time range (2020), provides wetland extent and location in the Irtysh River Basin but lacks detailed wetland characteristics. Conversely, GWL_FCS30, boasting high resolution (30 m) and multiple wetland types, captures intricate wetland details and ecological features but may not be optimal for long-term changes and global comparisons. ESA CCI-LC, with lower resolution (300 m) and a broader temporal scope, facilitates long-term changes and global comparisons but sacrifices detail in wetland characteristics and ecological features. Understanding these nuances enables judicious selection and application of RS products in diverse wetland monitoring and management scenarios.

4. Discussion

This study meticulously assessed the accuracy and consistency of eleven RS wetland products in extracting wetland information within the Irtysh River Basin. Our findings elucidate substantial differences in both wetland area and type among the various products, primarily attributed to factors such as data sources, spatial resolution, classification schemes, and production processes.

For instance, the GWL_FCS30 product, leveraging multi-source data, markedly enhances the identification of small-area wetlands, resulting in a wetland area almost 3.5 times larger than that identified by the AGLC-2015 product. Noteworthy is GWL_FCS30's adoption of a detailed wetland subtype division, revealing richer internal differences within wetlands. Furthermore, spatial patterns and morphological characteristics exhibited heterogeneity across different products, influenced by factors such as data sources, classification methods, and processing techniques. The GWL_FCS30 product excels in depicting intricate internal morphological features, presenting clearer and continuous boundary information.

The examination of indicators such as the similarity coefficient and Kappa coefficient revealed consistency in the primary wetland distribution areas across different products. However, the presence of significant "false differences" highlighted the impact of classification errors, possibly intensified by data uncertainty during the classification process.

Our research carries significant implications. Firstly, we propose a comprehensive framework and method for selecting and validating wetland products, applicable beyond wetlands to other land surface elements. This contribution provides valuable support for RS data evaluation and application. Secondly, our study illuminates the profound influence of data sources and methods on the quality of wetland information extraction. This insight not only guides the technical trajectory and research focus of relevant production institutions but also serves as a reference for the ongoing innovation and development of RS technology. Lastly, our comparative results offer practical guidance for government departments and research institutions, aiding in the selection of suitable wetland products for monitoring regional changes. This, in turn, provides crucial information and data for informed scientific decision-making, wetland protection, and management.

Nevertheless, our study is not without limitations. Primarily, our comparative analyses were confined to a specific watershed region, potentially limiting the generalizability of our results to different geographic environments. Additionally, the use of a limited validation sample hinders a comprehensive assessment of absolute classification accuracy. Further, the examination of products for a single year limits insights into their performance across temporal changes. Future research avenues involve expanding samples across diverse topographic regions, establishing a standardized large-sample validation database for comprehensive accuracy assessment, and introducing time-series products for a more nuanced understanding of wetland change dynamics. These expansions aim to deepen our understanding and exploration within this field, addressing identified limitations and bolstering the robustness of our findings.

5. Conclusions

This study undertook a comprehensive comparison and evaluation of RS wetland products within the Irtysh River Basin, with the overarching goal of furnishing a scientific basis for wetland protection and management. Meanwhile, it aims to offer valuable insights for the ongoing development of wetland RS monitoring technology. The analysis incorporated eleven global-scale land cover or wetland RS products, dissecting their disparities, advantages, and drawbacks in delineating wetland area, type, distribution, and consistency in the Irtysh River Basin. The ensuing conclusions are as follows:

1. Significant Disparities in Wetland Description: Considerable differences were observed in the depiction of wetlands within the Irtysh River Basin among various RS products, attributed to factors such as data sources, spatial resolution, classification schemes, algorithms, and validation methods. Notably, the GWL_FCS30 product exhibited the highest wetland area extraction, while the AGLC-2015 product yielded the lowest. GWL_FCS30 demonstrated an enhanced capacity to portray internal morphological features, presenting clearer and more continuous boundary information. The ESRI_Global-LULC_10m and FROM_GLC10_2017 products exhibited superior classification consistency;
2. Key Influencing Factors on Information Quality: Central to the precision of wetland information extraction in the Irtysh River Basin are the influencing factors of data sources, classification methods, and validation schemes. Achieving high-quality wetland products necessitates obtaining raw data with elevated spatial and temporal resolution through the fusion of multiple sources. It is imperative to establish a detailed and scientifically grounded local wetland classification system, employ effective methods to unlock the full value of the data, and adhere to standardized and scientifically rigorous validation schemes to ensure result reliability,
3. Guidance for Future Endeavors: This study serves as a pivotal guide and reference for the selection and optimization of subsequent wetland products. It contributes valuable insights for the ongoing innovation and development of RS technology, providing a robust data foundation for informed wetland protection and management decisions. Nonetheless, certain limitations, including a restricted sample area, inadequate validation samples, and the absence of time-series products, underscore the necessity for future expansion and refinement in subsequent studies.

In summary, this research advances wetland monitoring technologies and underscores the critical considerations pivotal for accurate wetland information extraction. While acknowledging the limitations, the study's significance lies in its potential to inform strategic decision-making for wetland conservation and management, thus bridging the gap between RS technology and practical applications. To fortify the study's impact, future efforts should focus on addressing the identified limitations, expanding the scope of analysis, and incorporating temporal dimensions through the inclusion of time-series products. This would further amplify the relevance and applicability of the study's findings.

Author Contributions: Conceptualization, K.L. and A.S.; methodology, K.L. and A.S.; software, K.L.; validation, K.L., A.S., J.A. and W.L.; resources, A.S. and J.A.; data curation, K.L.; writing—original draft preparation, K.L.; writing—review and editing, K.L., A.S., J.A. and W.L.; visualization, K.L.; supervision, A.S.; funding acquisition, A.S. and J.A. All authors have read and agreed to the published version of the manuscript.

Funding: This work was partially supported by the Xinjiang Third Scientific Expedition (2022xjkk0702) and the Western Young Scholars Program of the Chinese Academy of Sciences (2022-XBQNXZ-001).

Data Availability Statement: The research data used in this study is available from corresponding authors on request.

Acknowledgments: We would like to extend our gratitude to the following organizations for providing the remote sensing products utilized in this study: China National Centre for Basic Geographic Information, Copernicus Land Monitoring Service Global Team, ESRI Corporation, European Space Agency, Institute of Space and Astronautical Information Innovation of the Chinese Academy of Sciences, Gong Peng Team at Tsinghua University, NASA, European Union Joint Research Centre, and Sun Yat-sen University. We also wish to acknowledge the Google Earth Engine platform for facilitating aspects of the analysis. Finally, we sincerely appreciate the valuable comments from reviewers and editors, which significantly helped us to improve the quality of this manuscript.

Conflicts of Interest: The authors declare no conflicts of interest.

References

1. McCarthy, M.J.; Radabaugh, K.R.; Moyer, R.P.; Muller-Karger, F.E. Enabling efficient, large-scale high-spatial resolution wetland mapping using satellites. *Remote Sens. Environ.* **2018**, *208*, 189–201. [CrossRef]
2. Xi, Y.; Peng, S.; Ciais, P.; Chen, Y. Future impacts of climate change on inland Ramsar wetlands. *Nat. Clim. Chang.* **2020**, *11*, 45–51. [CrossRef]
3. Mao, D.; Wang, Z.; Du, B.; Li, L.; Tian, Y.; Jia, M.; Zeng, Y.; Song, K.; Jiang, M.; Wang, Y. National wetland mapping in China: A new product resulting from object-based and hierarchical classification of Landsat 8 OLI images. *ISPRS J. Photogramm. Remote Sens.* **2020**, *164*, 11–25. [CrossRef]
4. Fluet-Chouinard, E.; Stocker, B.D.; Zhang, Z.; Malhotra, A.; Melton, J.R.; Poulter, B.; Kaplan, J.O.; Goldewijk, K.K.; Siebert, S.; Minayeva, T.; et al. Extensive global wetland loss over the past three centuries. *Nature* **2023**, *614*, 281–286. [CrossRef] [PubMed]
5. Ludwig, C.; Walli, A.; Schleicher, C.; Weichselbaum, J.; Riffler, M. A highly automated algorithm for wetland detection using multi-temporal optical satellite data. *Remote Sens. Environ.* **2019**, *224*, 333–351. [CrossRef]
6. Hu, S.; Niu, Z.; Chen, Y. Global Wetland Datasets: A Review. *Wetlands* **2017**, *37*, 807–817. [CrossRef]
7. Davidson, N.C. How much wetland has the world lost? Long-term and recent trends in global wetland area. *Mar. Freshw. Res.* **2014**, *65*, 934–941. [CrossRef]
8. Jiang, W.; Wang, W.; Chen, Y.; Liu, J.; Tang, H.; Hou, P.; Yang, Y. Quantifying driving forces of urban wetlands change in Beijing City. *J. Geogr. Sci.* **2012**, *22*, 301–314. [CrossRef]
9. Cui, L.; Li, G.; Ouyang, N.; Mu, F.; Yan, F.; Zhang, Y.; Huang, X. Analyzing Coastal Wetland Degradation and its Key Restoration Technologies in the Coastal Area of Jiangsu, China. *Wetlands* **2018**, *38*, 525–537. [CrossRef]
10. Davidson, N.C.; Finlayson, C.M. Extent, regional distribution and changes in area of different classes of wetland. *Mar. Freshw. Res.* **2018**, *69*, 1525–1533. [CrossRef]
11. Zhao, Z.; Zhang, Y.; Liu, L.; Liu, F.; Zhang, H. Recent changes in wetlands on the Tibetan Plateau: A review. *J. Geogr. Sci.* **2015**, *25*, 879–896. [CrossRef]
12. Kim, S.G. The evolution of coastal wetland policy in developed countries and Korea. *Ocean Coast. Manag.* **2010**, *53*, 562–569. [CrossRef]
13. Let, M.; Pal, S. Socio-ecological well-being perspectives of wetland loss scenario: A review. *J. Environ. Manag.* **2023**, *326*, 116692. [CrossRef] [PubMed]
14. Brinson, M.M.; Malvárez, A.I. Temperate freshwater wetlands: Types, status, and threats. *Environ. Conserv.* **2002**, *29*, 115–133. [CrossRef]
15. Junk, W.J. Long-term environmental trends and the future of tropical wetlands. *Environ. Conserv.* **2003**, *29*, 414–435. [CrossRef]
16. Seifollahi-Aghmiuni, S.; Kalantari, Z.; Land, M.; Destouni, G. Change Drivers and Impacts in Arctic Wetland Landscapes—Literature Review and Gap Analysis. *Water* **2019**, *11*, 722. [CrossRef]
17. Chakraborty, S.K.; Sanyal, P.; Ray, R. Basics of Remote Sensing Techniques Applicable in Wetlands Ecosystems. In *Wetlands Ecology: Eco-Biological Uniqueness of a Ramsar Site (East Kolkata Wetlands, India)*; Springer: Berlin/Heidelberg, Germany, 2023; pp. 303–377.
18. Guo, M.; Li, J.; Sheng, C.; Xu, J.; Wu, L. A review of wetland remote sensing. *Sensors* **2017**, *17*, 777. [CrossRef]
19. Huang, Y.; Peng, J.; Chen, N.; Sun, W.; Du, Q.; Ren, K.; Huang, K. Cross-scene wetland mapping on hyperspectral remote sensing images using adversarial domain adaptation network. *ISPRS J. Photogramm. Remote Sens.* **2023**, *203*, 37–54. [CrossRef]
20. Betbeder, J.; Gond, V.; Frappart, F.; Baghdadi, N.N.; Briant, G.; Bartholomé, E. Mapping of Central Africa forested wetlands using remote sensing. *IEEE J. Sel. Top. Appl. Earth Obs. Remote Sens.* **2013**, *7*, 531–542. [CrossRef]
21. Kuleli, T.; Guneroglu, A.; Karsli, F.; Dihkan, M. Automatic detection of shoreline change on coastal Ramsar wetlands of Turkey. *Ocean Eng.* **2011**, *38*, 1141–1149. [CrossRef]
22. Wang, H.; Ma, M. Impacts of Climate Change and Anthropogenic Activities on the Ecological Restoration of Wetlands in the Arid Regions of China. *Energies* **2016**, *9*, 166. [CrossRef]
23. Chen, L.; Ren, C.; Zhang, B.; Li, L.; Wang, Z.; Song, K. Spatiotemporal Dynamics of Coastal Wetlands and Reclamation in the Yangtze Estuary During Past 50 Years (1960s–2015). *Chin. Geogr. Sci.* **2018**, *28*, 386–399. [CrossRef]
24. Wang, D.; Zhang, S.; Wang, G.; Liu, Y.; Wang, H.; Gu, J. Reservoir Regulation for Ecological Protection and Remediation: A Case Study of the Irtysh River Basin, China. *Int. J. Environ. Res. Public Health* **2022**, *19*, 11582. [CrossRef] [PubMed]

25. Hanchu, L.; Jie, F.; Baoyin, L.; Li, W.; Qin, Q. Practical Exploration of Ecological Restoration and Management of the Mountains-Rivers-Forests-Farmlands-Lakes-Grasslands System in the Irtysh River Basin in Altay, Xinjiang. *J. Resour. Ecol.* **2021**, *12*, 766–776. [CrossRef]
26. Huang, F.; Xia, Z.; Li, F.; Guo, L.; Yang, F. Hydrological Changes of the Irtysh River and the Possible Causes. *Water Resour. Manag.* **2012**, *26*, 3195–3208. [CrossRef]
27. Kingsford, R.T.; Basset, A.; Jackson, L. Wetlands: Conservation's poor cousins. *Aquat. Conserv. Mar. Freshw. Ecosyst.* **2016**, *26*, 892–916. [CrossRef]
28. Fan, J.; Abudumanan, A.; Wang, L.; Zhou, D.; Wang, Z.; Liu, H. Dynamic Assessment and Sustainability Strategies of Ecological Security in the Irtysh River Basin of Xinjiang, China. *Chin. Geogr. Sci.* **2023**, *33*, 393–409. [CrossRef]
29. Lehner, B.; Döll, P. Development and validation of a global database of lakes, reservoirs and wetlands. *J. Hydrol.* **2004**, *296*, 1–22. [CrossRef]
30. Gumbricht, T.; Roman-Cuesta, R.M.; Verchot, L.; Herold, M.; Wittmann, F.; Householder, E.; Herold, N.; Murdiyarso, D. An expert system model for mapping tropical wetlands and peatlands reveals South America as the largest contributor. *Glob. Chang. Biol.* **2017**, *23*, 3581–3599. [CrossRef]
31. Chen, G.; Jin, R.; Ye, Z.; Li, Q.; Gu, J.; Luo, M.; Luo, Y.; Christakos, G.; Morris, J.; He, J.; et al. Spatiotemporal Mapping of Salt Marshes in the Intertidal Zone of China during 1985–2019. *J. Remote Sens.* **2022**, *2022*, 9793626. [CrossRef]
32. Radelyuk, I.; Zhang, L.; Assanov, D.; Maratova, G.; Tussupova, K. A state-of-the-art and future perspectives of transboundary rivers in the cold climate–a systematic review of Irtysh River. *J. Hydrol. Reg. Stud.* **2022**, *42*, 101173. [CrossRef]
33. Jiang, S.; Yuan, Y.; Chen, F.; Shang, H.; Zhang, T.; Yu, S.; Qin, L.; Zhang, R. A 291 year precipitation reconstruction in the upper Irtysh River basin based on tree-ring width. *Acta Ecol. Sin.* **2016**, *36*, 2866–2875.
34. Hrkal, Z.; Gadalia, A.; Rigaudiere, P. Will the river Irtysh survive the year 2030? Impact of long-term unsuitable land use and water management of the upper stretch of the river catchment (North Kazakhstan). *Environ. Geol.* **2006**, *50*, 717–723. [CrossRef]
35. Jun, C.; Ban, Y.; Li, S. Open access to Earth land-cover map. *Nature* **2014**, *514*, 434. [CrossRef] [PubMed]
36. Buchhorn, M.; Smets, B.; Bertels, L.; De Roo, B.; Lesiv, M.; Tsendbazar, N.-E.; Herold, M.; Fritz, S. *Copernicus Global Land Service: Land Cover 100m: Collection 3: Epoch 2019: Globe. Version V3.0.1*; Laboratory of Geo-information Science and Remote Sensing: Wageningen, The Netherlands, 2020.
37. Karra, K.; Kontgis, C.; Statman-Weil, Z.; Mazzariello, J.C.; Mathis, M.; Brumby, S.P. Global land use/land cover with Sentinel 2 and deep learning. In Proceedings of the 2021 IEEE International Geoscience and Remote Sensing Symposium IGARSS, Brussels, Belgium, 11–16 July 2021; pp. 4704–4707.
38. Zanaga, D.; Van De Kerchove, R.; Daems, D.; De Keersmaecker, W.; Brockmann, C.; Kirches, G.; Wevers, J.; Cartus, O.; Santoro, M.; Fritz, S. ESA WorldCover 10 m 2021 v200. Zenodo 2022. Available online: https://zenodo.org/records/7254221 (accessed on 10 July 2023).
39. Zhang, X.; Liu, L.; Zhao, T.; Chen, X.; Lin, S.; Wang, J.; Mi, J.; Liu, W. GWL_FCS30: A global 30 m wetland map with a fine classification system using multi-sourced and time-series remote sensing imagery in 2020. *Earth Syst. Sci. Data* **2023**, *15*, 265–293. [CrossRef]
40. Gong, P.; Liu, H.; Zhang, M.; Li, C.; Wang, J.; Huang, H.; Clinton, N.; Ji, L.; Li, W.; Bai, Y.; et al. Stable classification with limited sample: Transferring a 30-m resolution sample set collected in 2015 to mapping 10-m resolution global land cover in 2017. *Sci. Bull.* **2019**, *64*, 370–373. [CrossRef] [PubMed]
41. Zhang, X.; Liu, L.; Chen, X.; Gao, Y.; Xie, S.; Mi, J. GLC_FCS30: Global land-cover product with fine classification system at 30 m using time-series Landsat imagery. *Earth Syst. Sci. Data* **2021**, *13*, 2753–2776. [CrossRef]
42. Harper, K.L.; Lamarche, C.; Hartley, A.; Peylin, P.; Ottlé, C.; Bastrikov, V.; San Martín, R.; Bohnenstengel, S.I.; Kirches, G.; Boettcher, M. A 29-year time series of annual 300-metre resolution plant functional type maps for climate models. *Earth Syst. Sci. Data Discuss.* **2022**, *2022*, 1–37.
43. Friedl, M.; Sulla-Menashe, D. MCD12Q1 MODIS/Terra+ aqua land cover type yearly L3 global 500m SIN grid V006. *NASA EOSDIS Land Process. DAAC* **2019**, *10*, 200.
44. Roy, P.; Agrawal, S.; Joshi, P.; Shukla, Y. *The Land Cover Map for Southern Asia for the Year 2000. GLC2000 Database*; European Commission Joint Research Centre: Brussels, Belgium, 2003.
45. Xu, X.; Li, B.; Liu, X.; Li, X.; Shi, Q. Mapping annual global land cover changes at a 30 m resolution from 2000 to 2015. *Natl. Remote Sens. Bull.* **2021**, *25*, 1896–1916.
46. Lu, D.; Weng, Q.; Moran, E.; Li, G.; Hetrick, S. Remote sensing image classification. *Adv. Environ. Remote Sens. Sens. Algorithms Appl.* **2011**, *9*, 219–240.
47. Real, R.; Vargas, J.M. The probabilistic basis of Jaccard's index of similarity. *Syst. Biol.* **1996**, *45*, 380–385. [CrossRef]
48. Congalton, R.G. A review of assessing the accuracy of classifications of remotely sensed data. *Remote Sens. Environ.* **1991**, *37*, 35–46. [CrossRef]
49. Jensen, J. Thematic information extraction: Image classification. In *Introductory Digital Image Processing: A Remote Sensing Perspective*; Pearson Education: London, UK, 1996; pp. 197–256.

50. Herold, M.; Mayaux, P.; Woodcock, C.; Baccini, A.; Schmullius, C. Some challenges in global land cover mapping: An assessment of agreement and accuracy in existing 1 km datasets. *Remote Sens. Environ.* **2008**, *112*, 2538–2556. [CrossRef]
51. Maxwell, A.E.; Warner, T.A.; Fang, F. Implementation of machine-learning classification in remote sensing: An applied review. *Int. J. Remote Sens.* **2018**, *39*, 2784–2817. [CrossRef]